



Calhoun: The NPS Institutional Archive
DSpace Repository

Theses and Dissertations

1. Thesis and Dissertation Collection, all items

1971

The effect of evaporated metallic electrodes
on the transition temperature of triglycine sulphate.

Pell, Richard Fairfax.

Monterey, California ; Naval Postgraduate School

<http://hdl.handle.net/10945/15682>

Downloaded from NPS Archive: Calhoun



<http://www.nps.edu/library>

Calhoun is the Naval Postgraduate School's public access digital repository for research materials and institutional publications created by the NPS community. Calhoun is named for Professor of Mathematics Guy K. Calhoun, NPS's first appointed -- and published -- scholarly author.

Dudley Knox Library / Naval Postgraduate School
411 Dyer Road / 1 University Circle
Monterey, California USA 93943

THE EFFECT OF EVAPORATED METALLIC
ELECTRODES ON THE
TRANSITION TEMPERATURE OF TRI-GLYCINE
SULPHATE

Richard Fairfax Pell



United States Naval Postgraduate School



THESIS

THE EFFECT OF EVAPORATED METALLIC ELECTRODES
ON THE
TRANSITION TEMPERATURE OF TRI-GLYCINE SULPHATE

by

Richard Fairfax Pell

Thesis Advisor:

William Reese

June 1971

Approved for public release; distribution unlimited.

The Effect of Evaporated Metallic Electrodes
on the
Transition Temperature of Tri-glycine Sulphate

by

Richard Fairfax Pell
Major, United States Army
B.S., West Virginia University 1960

Submitted in partial fulfillment of the
requirements for the degree of

MASTER OF SCIENCE IN PHYSICS

from the

NAVAL POSTGRADUATE SCHOOL
June 1971

Thesis
P 3274
c-1

ABSTRACT

Measurements of the effect of electrode thickness on the transition temperature of tri-glycine sulphate (TGS) are reported. An increase in the transition temperature is predicted utilizing the elastic Gibb's free energy equation of state. The prediction is verified by capacitance versus temperature measurements for evaporated gold electrodes varying in thickness from 250A to 3000A. The predicted increase in transition temperature is $.15^{\circ}\text{C}$ while the measured value is $.07^{\circ}\text{C}$.

TABLE OF CONTENTS

I.	THEORY-----	6
A.	INTRODUCTION-----	6
B.	THERMODYNAMIC MODEL-----	9
C.	ELECTRODE EFFECTS-----	12
D.	ELECTRODE EFFECTS IN TGS-----	16
II.	DESIGN OF EQUIPMENT-----	20
A.	GENERAL-----	20
B.	FURNACE-----	20
C.	EVAPORATION SYSTEM-----	25
D.	CAPACITANCE AND TEMPERATURE MEASUREMENTS-----	28
III.	PROCEDURE-----	29
A.	EVAPORATION-----	29
B.	SAMPLE PREPARATION-----	31
C.	OPERATIONAL PROCEDURE-----	31
IV.	DISCUSSION AND CONCLUSIONS-----	33
A.	DATA ANALYSIS-----	33
B.	DISCUSSION-----	35
C.	CONCLUSIONS-----	41
	LIST OF REFERENCES-----	43
	INITIAL DISTRIBUTION LIST-----	44
	FORM DD 1473-----	45

LIST OF TABLES

Table I. PROPERTIES OF TRI-GLYCINE SULPHATE-----19

Table II. MEASURED TRANSITION TEMPERATURES-----39

LIST OF FIGURES

1. Schematic Diagram of Equipment Used in Transition	
Temperature Measurements-----	21
2. Sketch of Sample Fixture Mounted on Base-----	23
3. Sketch of Evaporation Apparatus Located Inside Vacuum-	27
4. Reciprocal Capacitance Versus Temperature-----	34
5. Method of Determining Transition Temperature-----	37
6. Transition Temperature Versus Electrode Thickness-----	38

I. THEORY

A. INTRODUCTION

Ferroelectricity is the name applied to the phenomenon occurring in certain classes of dielectric materials which exhibit spontaneous, reversible polarization. The title is a historical one which draws upon the analogies between the effect of a coercive electric field upon a ferroelectric crystal and the effect of a coercive magnetic field upon a ferromagnetic material. The most prominent analogy is the hysteresis loop; however, there are other analogies such as: the presence of a Curie temperature θ , domain structure [4], and the Barkhausen effect [2].

The most important single characteristic of a ferroelectric crystal is the presence of a spontaneous, reversible polarization. Spontaneous polarization requires the presence of elemental dipoles; this requirement means that of the thirty-two classes of crystals, the eleven classes that have centers of symmetry cannot be ferroelectric, since no permanent dipole can be present in a symmetrical unit cell.

Of the twenty-one crystal classes which are non-centrosymmetric, twenty crystal classes exhibit piezoelectric effects. A piezoelectric crystal which is placed under external stress develops an electromotive force due to stress induced polarization. Furthermore, placing an electric field on a piezoelectric crystal produces a strain within the crystal which is dependent upon the direction

of the electric field. (Electrostriction which occurs in all materials is a strain proportional to the square of the electric field and is independent of the direction of the electric field.)

Ten of the twenty piezoelectric crystal classes are called polar crystals because they are spontaneously polarized. Surface charges or the pairing of dipoles normally causes an overall zero polarization for the entire crystal; therefore, the spontaneous polarization cannot be directly measured. The spontaneous polarization of these crystals is temperature dependent, and a change in polarization due to temperature changes can be measured. This temperature dependence of polar crystals is called the pyroelectric effect. One definition of a ferroelectric is a pyroelectric crystal which has reversible polarization.

It is possible to predict from symmetry properties alone that a crystal will possess both piezoelectric and pyroelectric properties. Ferroelectric properties cannot be predicted and must be determined by experimental methods.

Nearly all ferroelectric crystals possess a characteristic Curie temperature θ above which the crystal shows normal dielectric properties. For those few ferroelectric crystals which have no known Curie temperature, it is believed that the crystal is simply destroyed before the Curie temperature is reached. Guanidine aluminium sulphate hexahydrate is an example of a ferroelectric crystal which decomposes without reaching a Curie temperature [2].

Ferroelectric crystals in the temperature range where they exhibit spontaneous polarization are said to be in the ferroelectric phase. The other phase or normal dielectric phase is called the paraelectric phase, and the change of phase is called the transition.

X-ray diffraction and piezoelectric measurements have shown that at the transition the crystal structure changes from one of the polar classes (ferroelectric phase) to one of the non-polar classes (paraelectric phase).

In the paraelectric phase some of the physical parameters associated with the polar axis follow the Curie-Weiss law, $C/(T-\theta)$, where C is a constant which depends upon the parameter of interest, T is the temperature, and θ is defined as the Curie temperature which is normally assumed to be close to the transition temperature. The Curie-Weiss law predicts that in the neighborhood of the transition, the dielectric susceptibility, χ , associated with the polarization axis will approach infinity. Thus, capacitance measurements are a convenient measurement technique.

The behavior of observable parameters is quite similar for many ferroelectric materials; however, the microscopic behavior may be quite different. In barium titanate, for example, the transition is associated with a mechanical instability of certain transverse optical vibration modes. In other ferroelectrics, particularly those containing hydrogen bonds, the nature of the transition has not yet been definitively established; there is a more complex interplay between short range forces and the long range depolarization forces responsible for the transition in barium titanate.

B. THERMODYNAMIC MODEL

If the crystal is considered as a thermodynamic system, a model which adequately predicts the behavior of the crystal may be developed. The development of the model will be outlined here, and complete descriptions may be found in a number of references [1,2,4,6].

The internal energy density of a single domain piezoelectric crystal may be written:

$$du = Tds + \sum_{ij} X_{ij} x_{ij} + \vec{E} \cdot d\vec{P} \quad (1.a)$$

where u is the internal energy density, s the entropy density, T the temperature, X_{ij} is the stress, x_{ij} is the strain, \vec{E} is the electric field vector, and \vec{P} is the polarization vector. In the most general case X_{ij} and x_{ij} must be treated as tensors.

For the majority of ferroelectric crystals, the polarization axis may be assumed to coincide with one crystal axis so that only a single component of the P and E vectors need be considered. Furthermore, symmetry arguments allow one to reduce the stress and strain tensors when considering a specific crystal.

Assuming that all possible simplifications have been made, the equation for the internal energy density may be written:

$$du = Tds + EdP + X dx \quad (1.b)$$

where E and X now apply to external quantities, P and x refer to total quantities, and all tensor notation has been dropped for simplicity.

The application of Legendre transformations to the equation for internal energy allow equation (1.b) to be rewritten in free energy form. Of the four possibilities, the one selected for presentation here is the elastic Gibbs free energy since this form contains only non-singular coefficients:

$$dG_1 = - s dT + E dP - x dX . \quad (2)$$

From equation (2), an equation of state may be obtained by expanding the free energy function in terms of the natural variables. If small order effects are ignored, the equation of state is written:

$$G_1 = G_0 - S^P X^2 - b P X + \frac{1}{2} k^X P^2 \quad (3)$$

where the superscripts indicate the variable held constant: S is the elastic compliance constant, ($C = \frac{1}{S}$ where C is the elastic constant) b is the piezoelectric strain coefficient, and $k = \frac{1}{\chi}$ is the reciprocal dielectric susceptibility. In this form of the expansion all temperature dependence is assumed to be contained in the coefficients.

As written, equation (3) is adequate to describe piezoelectric but not ferroelectric behavior, since it does not yield spontaneous polarization. By the addition of a function, $f(P)$, containing higher order terms in P , equation (3) can be made to describe spontaneous polarization. By noting that the free energy should not be effected by a change in sign of the polarization, one may easily argue that $f(P)$ need only contain even powers of P .

The equation of state of a ferroelectric crystal is then written:

$$G = G_0 - \frac{1}{2} S^P X^2 - b P X + \frac{1}{2} k^X P^2 + \frac{1}{4} g_1 P^4 + \frac{1}{6} g_2 P^6 \quad (4)$$

where g_1 and g_2 are the expansion coefficients of P^4 and P^6 . The description of a second order transition requires only the term $\frac{1}{4} g_1 P^4$, but to describe a first order transition, both terms must be used.

By taking partial derivatives of equation (4) with respect to P , one finds expressions for the electric field E and the reciprocal susceptibility $\frac{1}{\chi}$ which permits testing of the model by experiment.

Confining the description to a ferroelectric material which undergoes a second order transition and taking the partial derivative with respect to P , the equation of the electric field is written:

$$E = - b X + \alpha(T-\theta)P + g_1 P^3 \quad (5)$$

where k^X has been replaced by the form containing temperature dependence.

If the crystal is further assumed to be free of external stresses, the equation becomes:

$$E = \alpha(T-\theta)P + g_1 P^3. \quad (6)$$

The reciprocal susceptibility is found by taking the partial derivative of E with respect to P :

$$\frac{1}{\chi} = \alpha(T-\theta) + 3g_1 P^2. \quad (7)$$

The value of the reciprocal susceptibility may be found directly from equation (7) for values above the transition, since in this range P is equal to zero. For values above the transition, $\frac{1}{\chi} = \alpha(T-\theta)$.

For values of the reciprocal susceptibility below the transition, equation (6) is solved for the square of the spontaneous polarization by assuming that P is the spontaneous polarization when E is equal to zero,

$$P^2 = - \frac{\alpha(T-\theta)}{g_1} \quad (8)$$

By substituting this value into equation (7) one determines the value of the reciprocal susceptibility below the transition to be $\frac{1}{\chi} = - 2\alpha(T-\theta)$.

When the crystal cannot be considered free of external stresses, for example, a crystal under hydrostatic pressure, equation (5) may be solved utilizing the stress components to predict an alteration of the Curie temperature. (In the case of a second order transition, the Curie temperature and the transition temperature are assumed to be identical.) Experimental results have verified this predicted shift in the Curie temperature [5].

C. ELECTRODE EFFECTS

It has been proposed that the evaporation of metallic electrodes on ferroelectric crystals may result in a clamping effect which alters the characteristics of the material. Jona and Shirane [4] suggest this clamping may in part be responsible for the differences

in the peak value of susceptibility reported for tri-glycine sulphate. Other effects which have been reported include different rates of electrically induced domain growth in barium titanate when gold electrodes were substituted for aqueous electrodes [2]. Benepe [1] has outlined a solution to the equation of state which predicts that the clamping effect of the electrodes could produce a shift in the Curie temperature.

Since the primary effect of electrode clamping would seem to involve the piezoelectric nature of ferroelectric crystals, two cases must be considered: Case 1, the crystal is piezoelectric in both phases; Case 2, the crystal is piezoelectric in only the ferroelectric phase. Rochelle salt is an example of case 1, while potassium di-hydrogen phosphate and tri-glycine sulphate are examples of case 2.

Assuming that the electrode is placed upon the crystal in the ferroelectric state and that the external stress caused by the electrode will obey Hooke's Law, the non-tensor form of the electrode stress can be written:

$$X_e = A(x_0 - x), \quad (9)$$

where X_e is the external stress due to the electrode, A is an effective elastic modulus for the electrode, x_0 is the strain during placement of the electrode, and x is the strain under any other condition. (Under the simplest conditions, x_0 is the spontaneous strain.)

Selecting the linear piezoelectric equation, $X = C^P x - aP$ which may be obtained from equation (3) and imposing the condition that during the placement of the electrodes $X = X_e$ and $x = x_o$, the equation for the electric field becomes:

$$E = - \frac{A C^P b x_o}{A + C^P} + \left(k^X + ab - \frac{ab}{A + C^P} \right) + g_1 P^3 . \quad (10)$$

If a , b , A , and C^P are assumed to be independent of the polarization, the equation may be written:

$$E = - E_o + [\alpha(T - \theta) + B]P + g_1 P^3 . \quad (11)$$

(Equation (11) has been simplified by writing the constant term $\frac{A C^P b x_o}{A + C^P}$ as E_o , the constant term $ab - \frac{ab}{A + C^P}$ as B , and also, the temperature dependence of k^X is now included.) It can be noted that except for the constant term B , the equation is the same as that of a ferroelectric subject to a bias field [2].

As previously discussed, ferroelectric behavior is characterized by a hysteresis loop, and the transition is described as the point where the crystal changes from ferroelectric to paraelectric behavior. To describe a hysteresis loop, then, the solutions of equation (11) must provide two unequal, real solutions for P .

Considering the cubic equation,

$$x^3 + ax + b = 0, \quad (12)$$

it is found that the solutions exist as follows:

$$\frac{b^2}{4} + \frac{a^3}{27} > 0 \quad \text{one real and two imaginary roots ;} \quad (13.a)$$

$$\frac{b^2}{4} + \frac{a^3}{27} = 0 \quad \text{three real roots with at least two equal roots;} \quad (13.b)$$

$$\frac{b^2}{4} + \frac{a^3}{27} < 0 \quad \text{three real and unequal roots.} \quad (13.c)$$

Comparing this result to equation (11) reveals that for $T > \theta + \frac{B}{\alpha}$ there can exist only one real solution. Furthermore, depending upon the values of E and E_o , there exists a series of solutions when $T < \theta + \frac{B}{\alpha}$ which have at least two values of P . The conclusion drawn is that the value $\theta + \frac{B}{\alpha}$ represents the transition temperature of a crystal subject to electrode clamping.

On the other hand, for at least some of the crystals which have only one piezoelectric phase, the piezoelectric effect is believed to be "induced" by electrostriction. Both barium titanate and tri-glycine sulphate belong to this group [3]. Under these circumstances the piezoelectric components can no longer be considered constant but must be considered as explicit functions of the spontaneous polarization. Proceeding with this assumption and writing the constant of proportionality as K , the piezoelectric stress and strain coefficients, a and b , can be related to the polarization as follows:

$$b = KP, \quad (14.a)$$

$$a = C^P b = C^P KP. \quad (14.b)$$

These relationships may then be substituted into equation (10).

The result is:

$$E = - E'_O P + \alpha(T-\theta)P + B'P^3 + g_1P^3. \quad (15)$$

In equation (15) the term

$$\frac{A C^P \times K}{A + C^P}$$

is written as E'_O , and the term

$$C^P K^2 - \frac{C^P K^2}{C^P + A}$$

is written as B' . Again setting E equal to zero and solving for the square of the spontaneous polarization and the reciprocal susceptibility:

$$P^2 = \frac{E'_O - \alpha(T-\theta)}{g_1 + B'}, \quad (16)$$

$$\frac{1}{\chi} = - E'_O + \alpha(T-\theta) + 3(B' + g_1)P^2. \quad (17)$$

When the value for P^2 given by equation (16) is substituted into equation (17), the reciprocal susceptibility becomes:

$$\frac{1}{\chi} = - 2\alpha(T-\theta - \frac{E'_O}{\alpha}) \quad (18)$$

where E'_O/α may now be interpreted as an effective increase in the Curie temperature.

D. ELECTRODE EFFECTS IN TGS

Tri-glycine sulphate (TGS) was selected as a convenient ferroelectric crystal for a test of the theory. TGS has a transition

temperature of approximately 49°C . Information concerning the various elastic and piezoelectric properties is available in the literature [3,5]. Table I lists some additional properties of TGS.

Ikeda et.al. [3] have measured the electrostrictive and piezoelastic properties of TGS and found that the relationship between b , the piezoelectric stress constant, and Q , the electrostrictive constant is:

$$b = 2QP. \quad (19)$$

Using the relationships now available and solving for $\Delta\theta$ yields:

$$\Delta\theta = \frac{AC^P}{A+C^P} \left(\frac{2Qx_o}{\alpha} \right). \quad (20)$$

To proceed with a numerical calculation requires certain assumptions concerning A and x_o .

A is assumed to be an effective elastic modulus and must certainly depend upon the material of the electrode; however, the value of A would be expected to be strongly dependent upon the thickness of the electrode for thin films and should also be dependent upon the structure of the electrode. In lieu of specific knowledge of A , the elastic stiffness constant of gold, a common electrode material, was chosen for a representative calculation.

To evaluate x_o , it was assumed that the electrode stress was zero when the electrode was placed upon the crystal. Equation (9) may then be solved for x_o in terms of the elastic constants and the polarization. (This assumption serves to simplify the calculation,

but if some knowledge of the electrode stress were available, that value could be used and would, in general, increase the value calculated for $\Delta\theta$.)

Using the relationships between a, b, and Q results in an equation for $\Delta\theta$ in which all parameters are known:

$$\Delta\theta = \frac{AC^P}{A+C^P} \left(\frac{4Q^2 P_o^2}{\alpha} \right) . \quad (21)$$

To complete the calculation, the following values were substituted into equation (21):

$$\begin{aligned} C^P &= 2 \times 10^{11} \text{ dyne/cm}^2 & P_o &= 8.4 \times 10^3 \text{ statcoulombs/cm}^2 \text{ (23}^\circ\text{C)} \\ A &= 4 \times 10^{11} \text{ dyne/cm}^2 & \alpha &= 4\pi/3200 \text{ (Kelvins)}^{-1} \\ Q &= .4 \times 10^{-11} \text{ c.g.s. units [3]} \end{aligned}$$

This calculation predicts that metallic gold electrodes on a TGS crystal will raise the observed transition temperature by .15°C over the temperature which would be observed for a "free" crystal.

TABLE I

Properties of Tri-glycine Sulphate (TGS)

Chemical Formula $(C_2NO_2H_5)_3 \cdot H_2SO_4$ Transition Temperature $49^\circ C$

Crystal Properties:	<u>Ferroelectric Phase</u>	<u>Paraelectric Phase</u>
Class	Polar-spheroidal	Monoclinic prismatic
Space group	$C_2^2-P_{21}$	$C_{2h}^2-P_{21}/m$
Lattice parameters	a' 9.15 Å b' 12.69 Å c' 5.73 Å β $105^\circ 40' \pm 20'$	

II. DESIGN OF EQUIPMENT

A. GENERAL

It was decided to attempt to measure electrode clamping effects by utilizing two TGS crystals at the same temperature. One crystal would have standard electrodes, and the thickness of the electrodes of the second crystal could be varied. The use of a crystal for control eliminated difficulties which might have arisen in attempting to calibrate thermometers to absolute values and minimized the possibility of interpreting extraneous phenomena as electrode clamping.

B. FURNACE

The furnace which held the samples was designed to operate in a vacuum so that convective losses and heat gradients could be minimized. This design permitted the use of small heating elements powered by a direct-current electronic power supply.

The furnace consisted of a thick-walled aluminum tube, closed at the top, with a sliding fit at the bottom to allow access to the sample fixture. The furnace was wrapped over all surfaces with .005 inch diameter manganin wire which served as the heating element. The wire was wound in proportion to the surface area, and provision for trimming sections of the heater to control gradients was included in the design. (See Figure 1.) The entire furnace was attached to a baseplate by a ceramic link which provided electrical and thermal insulation.

The fixture which held the samples consisted of a vertical aluminum plate and phosphor bronze clips mounted on a circular

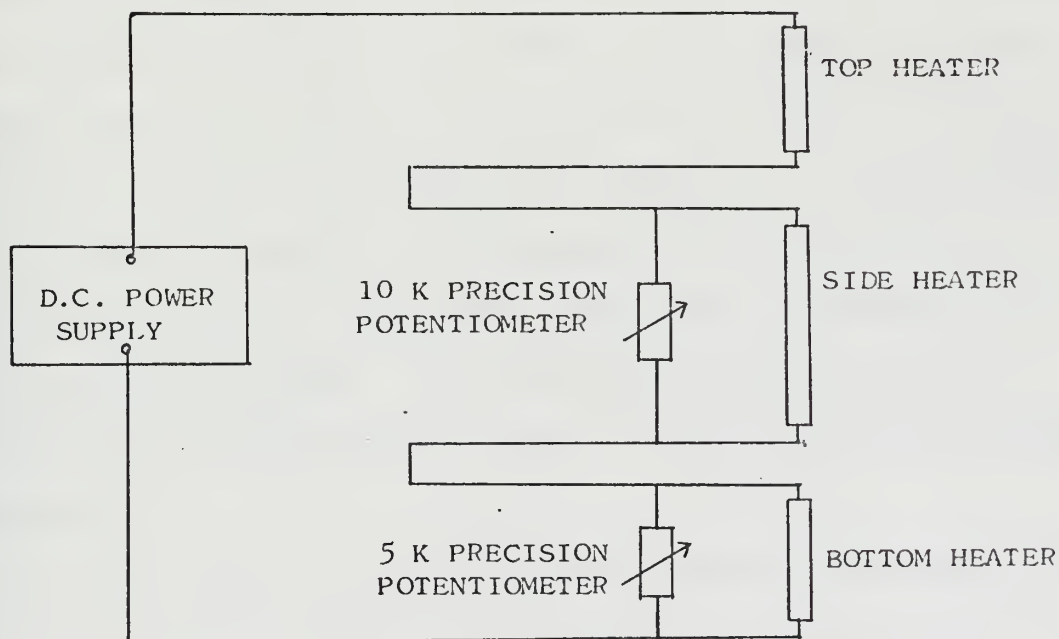
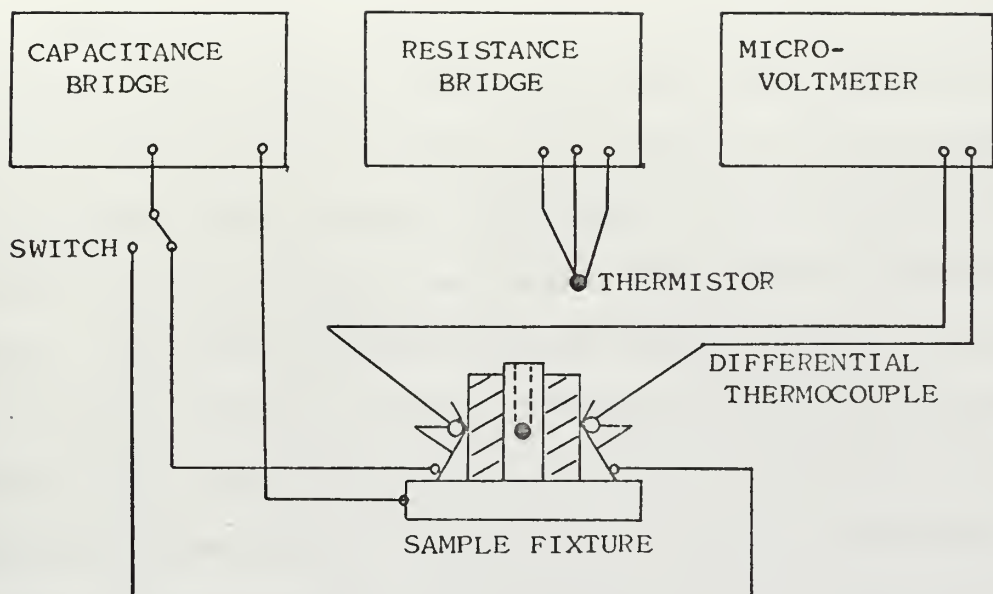


Figure 1. Schematic Diagram of Equipment Used in Transition Temperature Measurements

block. Figure 2 shows a side view of the fixture mounted inside the furnace. The phosphor bronze clips were electrically insulated from the rest of the fixture and served as one of the electrode contacts. The portion of the clip which made contact with the electrode of the crystal was faced with indium to improve the contact. The vertical aluminum block served as a heat sink and as the common electrode contact. The bearing area of the aluminum block was also faced with indium to minimize the effects of irregularities in mating the surface of the crystal to the block. The fixture was attached to the remainder of the furnace by a brass thermal link.

The furnace was instrumented with four YSI precision thermistors and a differential thermocouple. Three of the thermistors were arranged around the interior of the furnace as a check on thermal gradients. The fourth thermistor was inserted in a close fitting hole drilled in the center of the aluminum plate to which the samples were attached. The sample temperature was assumed to be the same as the aluminum. The differential thermocouple was attached to the phosphor bronze clips to sense any gradient between the samples.

The thermistors on the interior walls of the furnace were provided with a copper foil heat sink attached to the leads and cemented to a small piece of synthetic mica. The thermistor utilized to sense the sample temperature was carefully fitted in the hole, and heat conducting grease was used to assure adequate

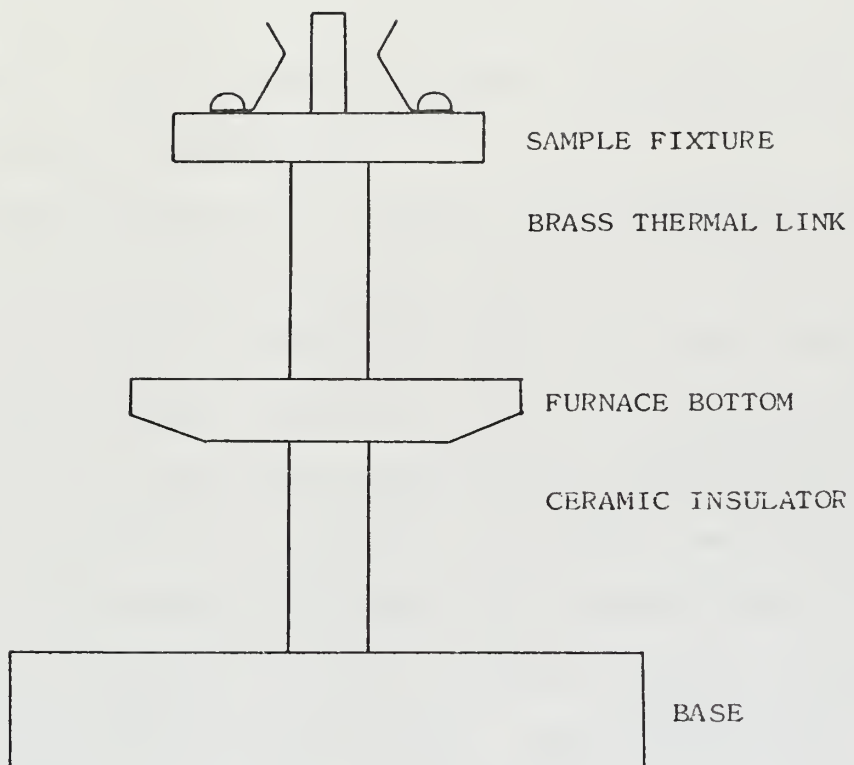


Figure 2. Sketch of Sample Fixture Mounted on Base

thermal contact. The thermocouple junctions were also mounted on synthetic mica which in turn was cemented to the phosphor bronze clips.

Manganin wire was used to attach the thermistor leads to a standard vacuum feedthrough. The thermocouple was copper-constantan with the constantan being the short link joining the two junctions, and the copper leads were brought to the exterior using standard thermocouple feedthroughs.

Prior to being mounted in the furnace, the thermistors were tested. All four were placed as nearly as possible in thermal contact, and the bundle was packed in a tube using heat-conducting grease. The tube was then immersed in a bath. All thermistors were found to be well within the manufacturer's specifications.

After the thermistors were mounted, the furnace was placed in the vacuum, and the temperature brought up to approximately 49°C . The trimmer potentiometers were then adjusted to minimize thermal gradients in the interior of the furnace. Some difficulty was experienced initially, since the system tended to be as much as $.5^{\circ}\text{C}$ cooler on the top. This problem was eliminated by fabricating a heat reflecting shield of aluminum foil over the top of the furnace. With the heat shield in place, the furnace was brought into equilibrium.

The relatively massive nature of the fixture, combined with the large contact area of the crystal tended to assure thermal equilibrium between the block and the crystal. The disadvantage of such an arrangement is the long thermal response time involved.

For this system, the thermal response time was in the neighborhood of three minutes. Because of the long thermal response time, no attempt was made to design an automatic controller, and all temperature control was performed manually.

C. EVAPORATION SYSTEM

The electrodes investigated were evaporated metallic films of varying thickness. This type of electrode is commonly used and offered the advantage of ease in monitoring and controlling thickness.

An NRC-3372 High Vacuum System was modified to provide both evaporation facilities and the vacuum chamber for the testing of samples. The basic system was comprised of a 15 CFM mechanical pump and a four-stage, 6 inch fractionating oil diffusion pump. The remainder of the system included: an 18 inch diameter bell-jar and electrical hoist; a liquid nitrogen cold trap; and a feed-through collar. The vacuum gauging consisted of two Hastings-Raydist thermocouple gauges and one Veeco hot filament ionization vacuum gauge. The gauges were controlled and read by a Consolidated Vacuum Products combination thermocouple-ionization gauge control.

The evaporation power was provided by a 2 KVA current transformer driven by a 20 ampere variable autotransformer. The variable transformer was used to control the current to the filament. This system was capable of continuous currents of 180 amperes and peak currents of 250 amperes.

To minimize contamination of the bell-jar and furnace, the evaporation electrodes and source were inclosed in an aluminum chassis box which had been modified for this purpose. (See Figure 3.) The electrodes were fed into the aluminum box through .25 inch teflon sheet which provided electrical insulation. A hole cut in the top of the box confined the vaporized metal into a beam, and a second hole cut in the side permitted viewing of the filament.

A water-cooled, electrically operated shutter allowed the thickness of the evaporated material to be closely controlled and, further, prevented heating of the substrate during warm-up. The shutter mechanism was fabricated from a rotary solenoid of the type commonly used in automatic controls of rotary switches.

The thickness of deposited metal was continuously monitored by a Sloan DTM-3 Thickness Monitor. To monitor thickness, the DTM-3 employs a sensor head consisting of a 5 MHz quartz crystal oscillator installed in the vacuum, facing and exposed to the source. As the evaporant builds upon the surface of the crystal, its frequency changes. This changing signal is compared to a tunable reference oscillator located in the control unit. The demodulated beat frequency is used to provide an audio signal and a visual readout. The visual readout consists of a micro-ammeter calibrated in hertz. The changes in frequency indicated by the meter are then converted to thickness in angstrom units by use of the relationship;

$$\Delta f = \frac{DT}{2}$$

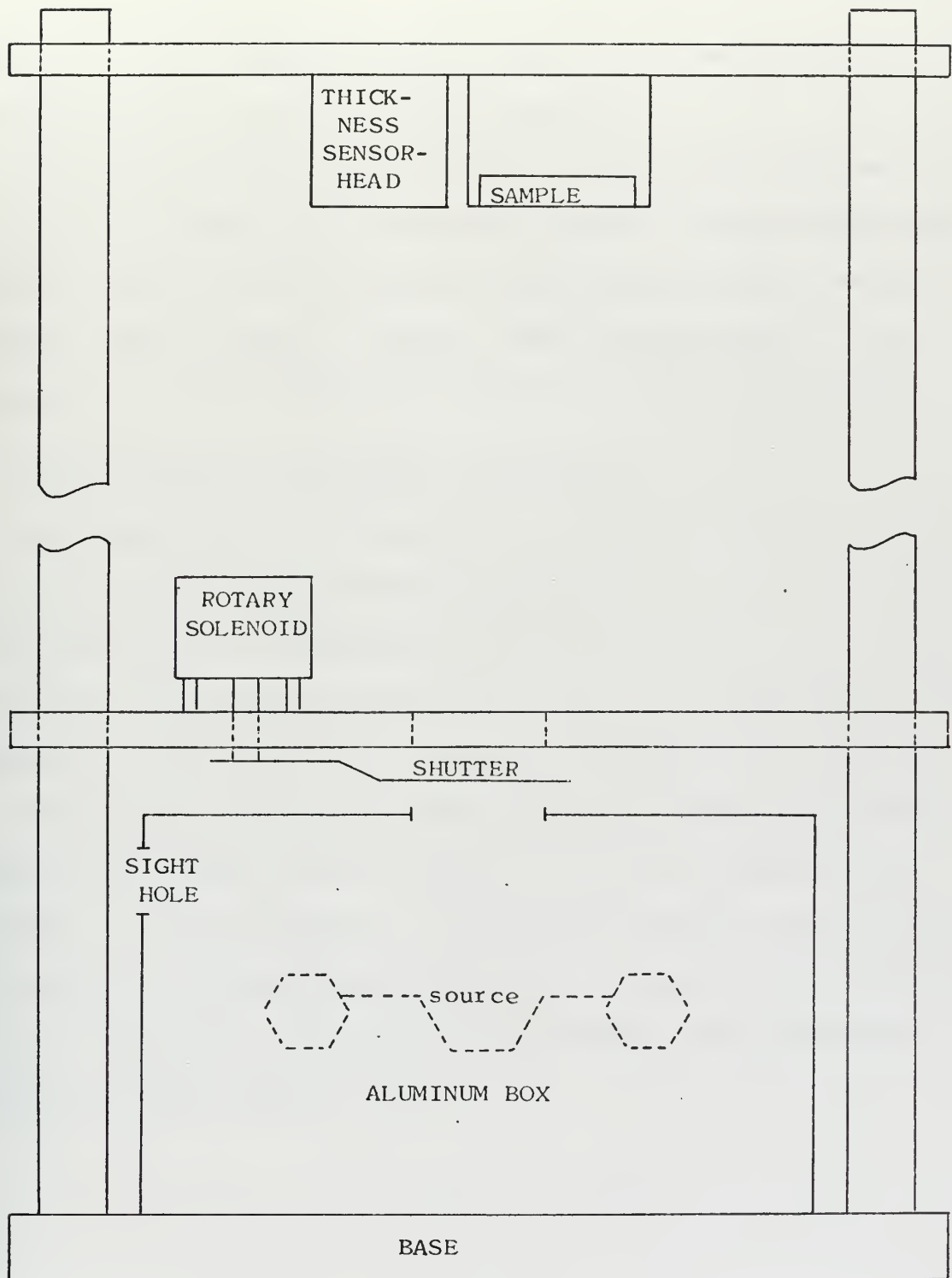


Figure 3. Sketch of Evaporation Apparatus Located in Vacuum.

where Δf is the frequency change in hertz, D is the density in gm/cm^3 , and T is the thickness in angstroms.

The fixture holding the substrate and the sensor head were co-planarly mounted on a sliding plate which allowed the distance between the source and the substrate to be continuously varied between 5 and 20 inches. Figure 3 shows the components of the evaporation system which were placed inside the vacuum system.

D. CAPACITANCE AND TEMPERATURE MEASUREMENTS

The resistance of the thermistors was measured with a locally built, low power bridge which was driven by a 317 Hertz oscillator. The thermistors were connected by a two lead method which essentially eliminated lead resistance from the circuit. The differential thermocouple was monitored with a Keithley 149 Milli-Microvoltmeter.

Capacitance measurements were made with a General Radio 716-C Capacitance Bridge driven at 1000 Hertz and utilizing an oscilloscope as a null indicator. A reversing switch was used to provide rapid switching between the samples. Figure 1 is a schematic drawing of the major components used in making capacitance and temperature measurements.

III. PROCEDURE

A. EVAPORATION

One of the first problems requiring solution was the development of evaporation techniques. Previous experience in this laboratory had indicated that films in the neighborhood of 1000\AA were required to assure continuity of the film. However, experience gained during this project indicated that continuous films of 500\AA could be produced routinely, and that with careful preparation and deposit, 250\AA continuous films could be produced.

After cleaving and string-sawing the crystal to produce rectangular plates, the surfaces of the plates were prepared by final polishing using Fisher 3/0 Metallographic Emory Paper with alcohol as a wetting and cleansing agent. Although the surface of crystals which had been polished with water-dampened tissue paper appeared to be smoother than those polished with abrasive, the abrasive method consistently produced higher quality films. It should be noted that the quality of the film was judged primarily on electrical properties and to a much lesser extent upon appearance. The presence of gaps in a poor quality film tended to lower the measured capacitance.

After preparation, the crystal was masked and placed in a holder above the source. Evaporations were performed at a pressure of 4×10^{-6} torr or less. The source could be observed through a hole cut in the side of the aluminum chassis box for that purpose. The

source current was raised to a point which caused a low incandescence, and the source and charge allowed to soak for 2 to 5 minutes at this current. After the soak, the current was again raised to the point where the charge wetted the filament. The charge was then carefully observed until a swirling of the charge material was noted. At this point, the shutter was opened, and the vaporized metal allowed to deposit the desired thickness on the substrate. A relay contained in the Sloan DTM 3 automatically interrupted the shutter current at a predetermined thickness.

Of the large variety of evaporation sources available the most satisfactory results were obtained by using plain metallic boats which were of the trough type, rather than the round dimple type. The use of this type of boat may be one of the primary reasons for the improved quality of films found during this investigation. The dimple source appears as essentially a point source at the surface of the substrate; small scratches or other irregularities in the surface then tend to have areas of shadow. The longer trough boat provides a finite source, and a much deeper scratch is required to produce an area which is totally in a shadow.

The boat material used most often with gold was tungsten, although molybdenum and tantalum were both tested with good results. Al_2O_3 coated boats tended to give the same difficulty as the single dimple boat; the charge remained beaded and did not fill the trough. In addition, the Al_2O_3 was very sensitive to thermal shock and required extra efforts in heating and cooling to prevent fracture.

The procedures used in evaporating tin, aluminum and gold were as outlined above. The primary difference in evaporating chromium was the use of a tungsten coated rod source supplied by the R.D. Mathis Company.

B. SAMPLE PREPARATION

Samples selected for use were consecutive cuts from a single crystal grown from an aqueous solution. After cleaving, the samples were string-sawed into rectangular plates. The surface area of the samples was approximately 1.6 cm^2 and the thickness varied from .20 to .28 cm. The surfaces of the samples were prepared, and 500A gold electrodes were evaporated on both faces. Initial runs were then made to determine the transition temperature. Following the initial runs, one sample was used as the control while the electrode thickness of the other was varied.

C. OPERATIONAL PROCEDURE

After placing the samples in the fixture, the furnace was closed and the chamber evacuated. The temperature of the samples was then raised to approximately 47°C . To conduct a "run", the heater current was raised to initiate heating.

The procedure used in taking data was to set a value on the resistance bridge and continuously balance the capacitance bridge as the capacitance increased. The value of capacitance recorded was the value at the time the null indicator of the resistance bridge reached the equilibrium position. The capacitance bridge was then switched to the other sample, and the bridge again

balanced. The second reading taken, which was in all cases the control sample, was subject to greater error than the first reading since the bridge had to be set to a new balance.

Capacitance measurements were made at intervals of 20 ohms well away from the transition and at intervals of 10 ohms in the neighborhood of the transition. A variation of 10 ohms in this range corresponded to a temperature change of approximately $.02^{\circ}\text{C}$. Due to the design of the furnace, the rate of heating or cooling could be varied, but it was not possible to hold the run at any particular temperature.

IV. DISCUSSION AND CONCLUSIONS

A. DATA ANALYSIS

During the initial phase of the investigation, data was analyzed by plotting the results in the form of reciprocal capacitance versus temperature. (Figure 4.) The points for these plots were obtained by subtracting the lead and stray capacitance (designated C_o) from the measured values and taking the reciprocal. The values of temperature were obtained by fitting the resistance versus temperature characteristic of the thermistor to an exponential curve. The equation used was of the form:

$$T = N \ln \frac{R}{R_o}$$

with T being the temperature in degrees Celsius; R, the measured value of resistance in kohms, and; R_o and N were constant parameters. The value used for R_o was 72.590 kohms, and 26.463 °C was used for N.

A program was written for the Hewlett-Packard desk computer which converted the data taken to the values of $\frac{1}{C-C_o}$ and T which were plotted. The curves shown in Figure 4 are representative of the results obtained during this investigation. The ordinate of the curves is plotted in terms of reciprocal capacitance; the capacitance of fixture plus stray lead capacitance has been subtracted from the measured value. The abscissa is plotted in degrees Celsius. Capacitance is directly proportional to susceptibility, so that the curves presented are entirely equivalent to plots of reciprocal susceptibility versus temperature.

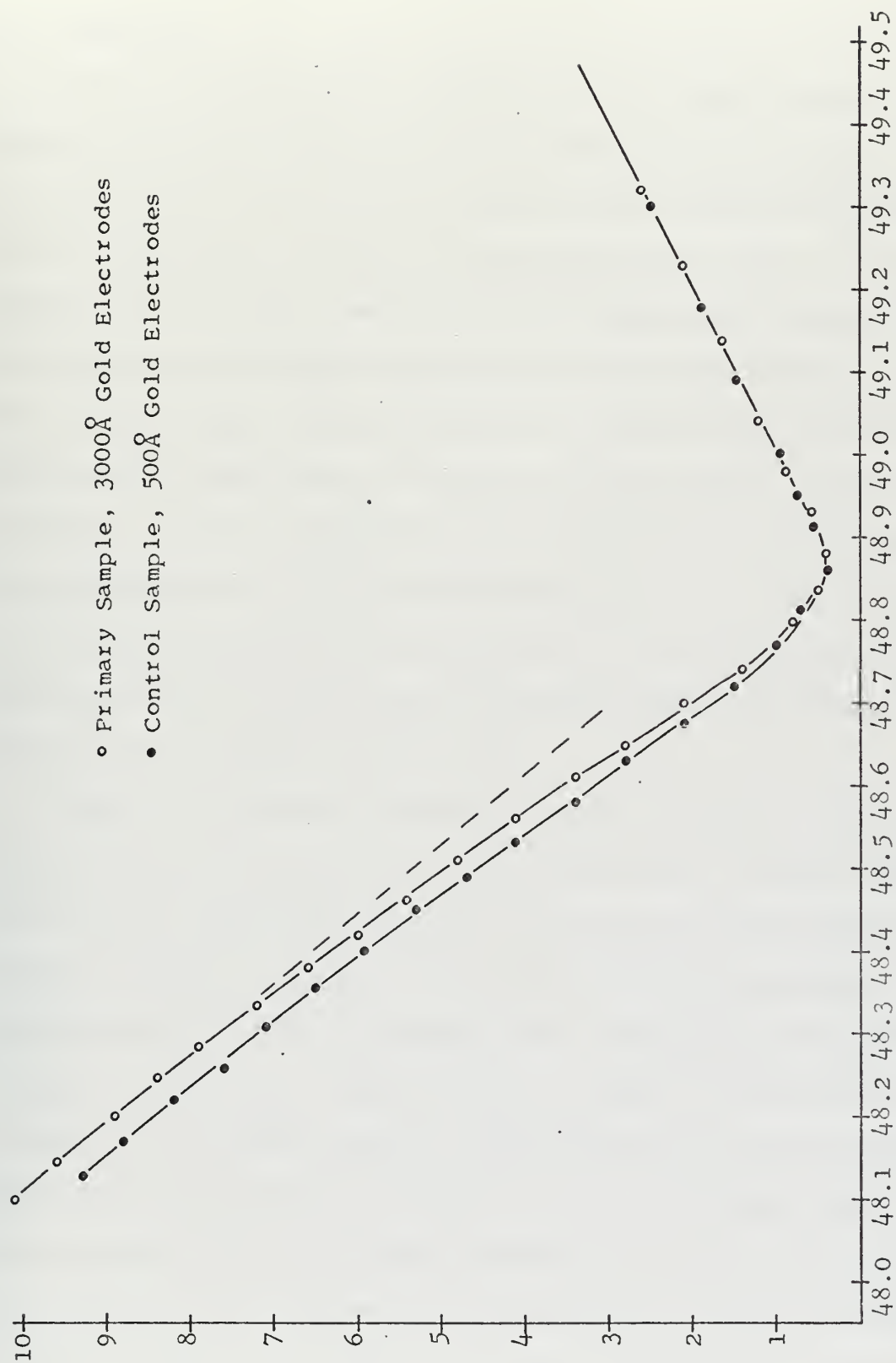


Figure 4. Reciprocal Capacitance Versus Temperature.

B. DISCUSSION

The thermodynamic model presented in the Theory portion of this paper predicts that the ratio of the slope of the reciprocal susceptibility versus temperature curves above the transition should be 2 to 1. The results of this investigation gave ratios of approximately 2.7 to 1. One simple correction that may be applied is the correction for the conditions under which the measurement was made. That is, the theory assumes isothermal conditions while measurements made at 1000 Hertz in the ferroelectric phase are more nearly adiabatic. If the correction is made for adiabatic measurement, the predicted ratio of slopes becomes 2.4 to 1. In most cases, experimental values are more nearly 2.7 to 1 as found by this investigation with the remaining discrepancy being considered a possible effect of domain clamping [4].

Figure 4 also shows a decided increase in slope as the temperature nears the transition. By extending the straight line drawn through the points well away from the transition and intersecting a similar line drawn for points near the transition, a temperature of 48.4°C is obtained. This temperature was generally constant for all runs. The increase in slope is also believed to be a result of the domain nature of ferroelectrics, and the conditions under which measurements were made. As was previously noted, the data was taken during continuous heating. The rate of heating was approximately 0.025 degrees per minute and was constant throughout the run. It has been shown that in the neighborhood of the transition the time-constant for thermally induced depolarization

becomes very long [7]. The effect may be caused by pinning of the domain walls on imperfections or by other mechanisms. The result is that as the time constant for thermally induced depolarization surpasses the rate of heating, and a lag occurs in the rate of depolarization.

The non-constant slope of the reciprocal capacitance curves in the ferroelectric phase coupled with the normal rounding at the transition caused difficulty in attempting to determine the transition temperature from this type of analysis. The other common method of determining the transition temperature is to assume that the transition occurs at the point of maximum capacitance. For the purpose of this discussion, the second definition was chosen. Figure 5 is a typical determination of the transition temperature (resistance).

Figure 6 is a plot of the measured values of transition temperature versus electrode thickness in angstroms. The general form of the curve is exponential which might be predicted since the relaxation thickness of the electrode material is a determining factor. An extrapolation of the curve to the point of zero electrode thickness gives a transition temperature of 48.80°C while the value measured with gold electrodes of 3000\AA was approximately 48.87°C . This apparent rise in transition temperature is $.07^{\circ}\text{C}$ as compared to the value calculated from theory of $.15^{\circ}\text{C}$. Table II is a listing of measured transition temperatures for various electrode thickness.

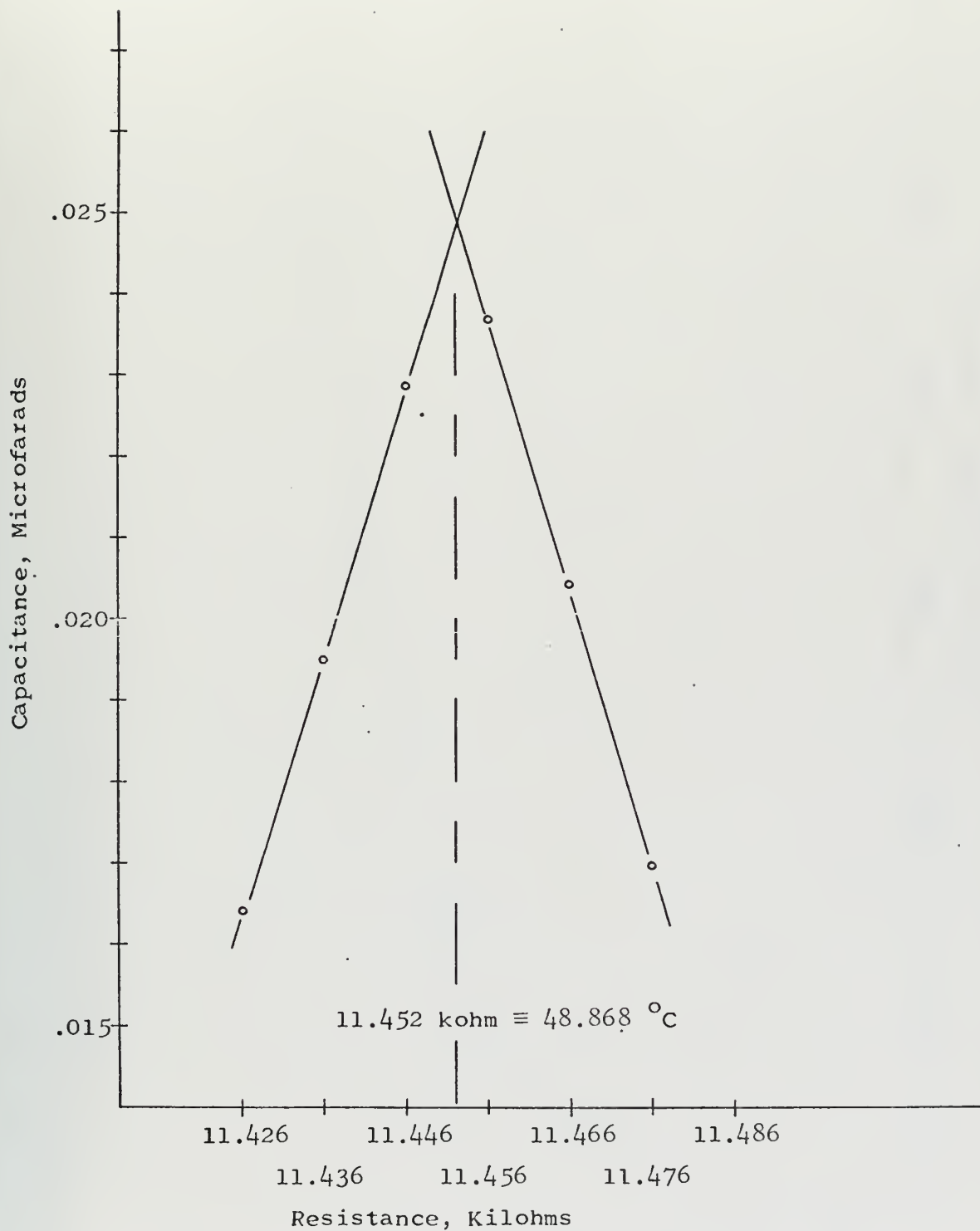


Figure 5. Method of Determining Transition Temperature.

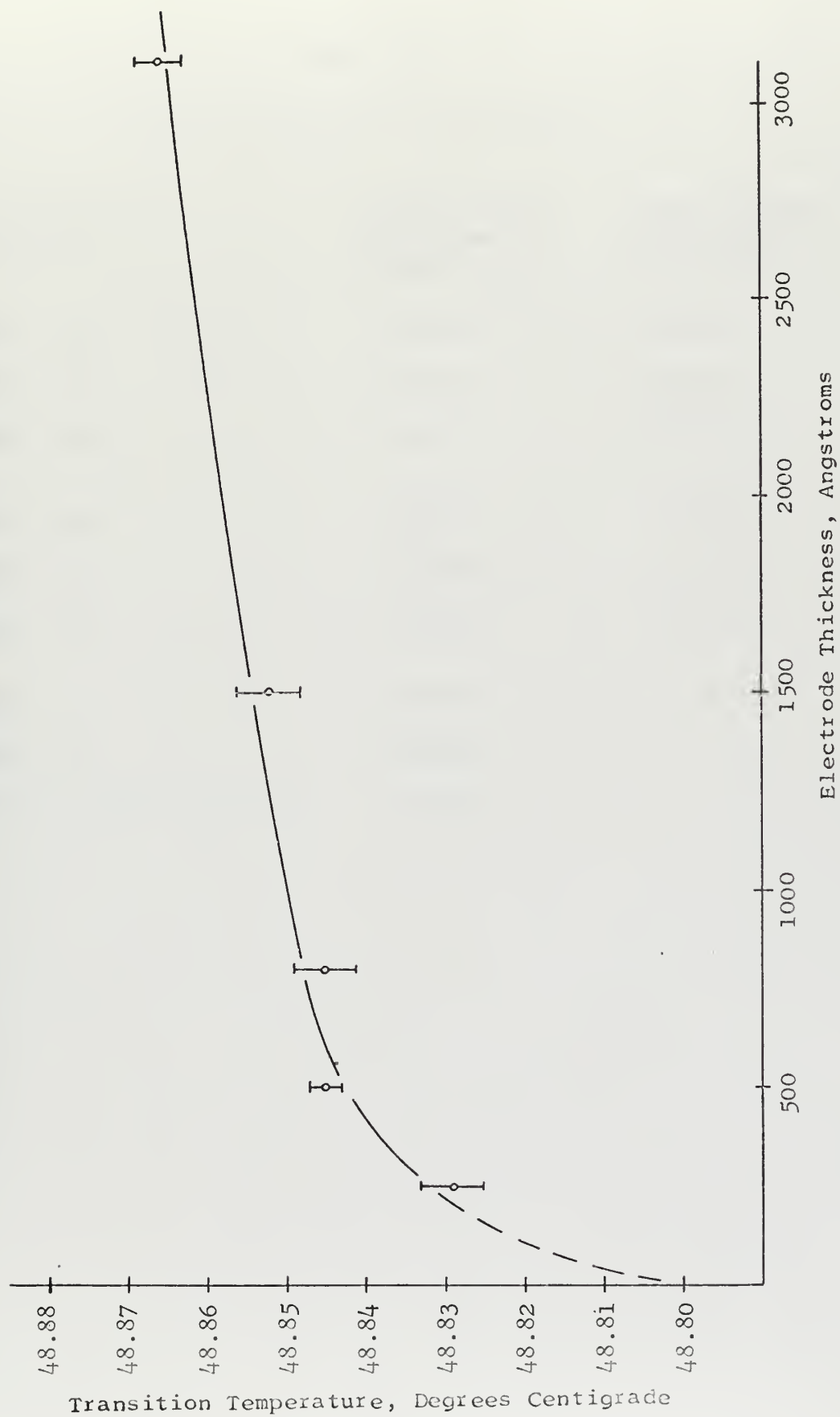


Figure 6. Transition Temperature Versus Electrode Thickness.

TABLE II

Measured Transition Temperatures

Film Thickness and Type		Primary Sample Transition Temperature °C	Control Sample Transition Temperature °C
500A	Au	48.845	48.831
500A	Au	48.847	48.833
500A	Au	48.843	48.840
1500A	Au	48.852	48.829
3000A	Au	48.864	48.840
3000A	Au	48.868	48.838
250A	Au	48.829	
800A	Au	48.845	
Silver conducting paint		48.852	

From Table II it may be noted that the measured transition temperature for the control crystal is not as consistent as the values measured for the primary sample. The reason for this variation has been previously discussed, and was a result of required experimental procedure. It is, apparent, however, that the control crystal exhibited no pattern of increased transition temperature as did the sample upon which electrode thickness was varied.

The possibility that the effect seen may have been a result of aging of the crystal or thermistor, or of shifts in the operating point of the bridge is further nullified by noting that the values measured at 250A and 800A were measured after the measurements at 500A, 1500A, and 3000A.

A fortunate accident during the investigation provided further indication that the crystals being tested did experience spontaneous strain, and that relative motion between the electrode and the contact was taking place. During the removal of a crystal from the fixture, a small amount of a rosin used as the core of an electronic solder was inadvertently smeared on the surface of the electrode contact. When the next run was made, the dissipation factor became quite high (.25 to .40) as the temperature approached the transition temperature. On all previous runs, this factor had been essentially zero. After the presence of the rosin was discovered, the fixture was cleaned with acetone, and the dissipation returned to zero. The effect was purposely reproduced with the other crystal. The effect was interpreted as mechanical losses taking place in the rosin.

The assumption that the crystal temperature during evaporation was approximately 23°C was checked by attaching a thermistor to the opposite face of a crystal and conducting an evaporation. The temperature of the bulk crystal was essentially unaffected by the evaporation. No such evaluation of the face receiving the evaporant was made.

A run made using silver conducting paint electrodes (a commonly used material) gave the same transition temperature (48.852°C) as was measured for 1500A gold electrodes. Caution must be exercised in attempting to correlate the results directly. A direct correlation requires tacit assumptions concerning polarization during electrode placement and relaxation thicknesses which have not been verified by this investigation.

C. CONCLUSIONS

The effect of gold electrodes evaporated on a TGS crystal in the ferroelectric state is to raise the transition temperature of the crystal due to electrode clamping. A rather rough calculation using the equation of state provides suprisingly accurate estimates of the increased transition temperature. From the data presented the relaxation thickness of evaporated gold films may be estimated as 400-600A.

This study should be continued to determine if the difference in calculated and measured values can be resolved. In particular, the study should attempt to determine if the error lies in the estimate

that the stress is zero at the time of electrode placement, or if the error is in the effective elastic modulus. In addition the study should determine through heat capacity and other measurements which parameters are effected by electrode thickness.

LIST OF REFERENCES

1. Benepe, J.W., Measurements of the Spontaneous Polarization in KH_2PO_4 , Ph.D. Thesis, Naval Postgraduate School, Monterey, California, 1970.
2. Fatuzzo, E. and Merz, W.J., Selected Topics in Solid State Physics, Volume VII, Ferroelectricity, Interscience Publishers, 1967.
3. Ikeda, T., Yoichi, T., and Toyoda, H., "Piezoelectric Properties of Triglycine-Sulphate," Japanese Journal of Applied Physics, Vol 1, No. 1, pages 13-21, July, 1962.
4. Jona, F., and Shirane, G., Ferroelectric Crystals, MacMillian, 1962.
5. Jona, F., and Shirane, G., "Effect of Hydrostatic Pressure on the Ferroelectric Properties of Tri-Glycine Sulfate and Selenate", Physical Review, Vol. 117, No. 1, Jan 1960.
6. Kittel, C., Introduction to Solid State Physics, 2nd Ed., John Wiley & Sons, 1965.
7. Schacher, E., Domain Switching Induced Temperature Instabilities in Ferroelectric Tri-Glycine Sulfate, Physics Letters, Vol. 28A, No. 8, Jan 1969.

INITIAL DISTRIBUTION LIST

	No. Copies
1. Defense Documentation Center Cameron Station Alexandria, Virginia 22314	2
2. Library, Code 0212 Naval Postgraduate School Monterey, California 93940	2
3. Assoc. Prof. W. Reese, Code 61Rc Department of Physics Naval Postgraduate School Monterey, California 93940	1
4. MAJ Richard F. Pell, USA Directorate of D.L. and P. USAARMS Fort Knox, Kentucky 40121	1

DOCUMENT CONTROL DATA - R & D

(Security classification of title, body of abstract and indexing annotation must be entered when the overall report is classified)

1. ORIGINATING ACTIVITY (Corporate author)

Naval Postgraduate School
Monterey, California 93940

2a. REPORT SECURITY CLASSIFICATION

Unclassified

2b. GROUP

3. REPORT TITLE

The Effect of Evaporated Metallic Electrodes on the Transition Temperature of Tri-glycine Sulphate

4. DESCRIPTIVE NOTES (Type of report and, inclusive dates)

Master's Thesis; June 1971

5. AUTHOR(S) (First name, middle initial, last name)

Richard F. Pell

6. REPORT DATE

June 1971

7a. TOTAL NO. OF PAGES

46

7b. NO. OF REFS

7

8a. CONTRACT OR GRANT NO.

b. PROJECT NO.

c.

d.

9a. ORIGINATOR'S REPORT NUMBER(S)

9b. OTHER REPORT NO(S) (Any other numbers that may be assigned this report)

10. DISTRIBUTION STATEMENT

Approved for public release; distribution unlimited.

11. SUPPLEMENTARY NOTES

12. SPONSORING MILITARY ACTIVITY

Naval Postgraduate School
Monterey, California 93940

13. ABSTRACT

Measurements of the effect of electrode thickness on the transition temperature of tri-glycine sulphate (TGS) are reported. An increase in the transition temperature is predicted utilizing the elastic Gibb's free energy equation of state. The prediction is verified by capacitance versus temperature measurements for evaporated gold electrodes varying in thickness from 250A to 3000A. The predicted increase in transition temperature is .15°C while the measured value is .07°C.

- tri-glycine sulphate (TGS)
- ferroelectric
- piezoelectric
- electrostriction
- electrode clamping
- electrode effects

Thesis
P3274
c.1

Pell

128453

The effect of evaporated metallic electrodes on the transition temperature of tri-glycine sulphate.

Thesis
P3274
c.1

Pell

128453

The effect of evaporated metallic electrodes on the transition temperature of tri-glycine sulphate.

thesP3274

The effect of evaporated metallic electr



3 2768 001 97933 9

DUDLEY KNOX LIBRARY